Solar Energy Materials & Solar Cells 94 (2010) 317–322

Contents lists available at ScienceDirect

Solar Energy Materials & Solar Cells

journal homepage: www.elsevier.com/locate/solmat

Dye-sensitized solar tubes: A new solar cell design for efficient current collection and improved cell sealing

Zion Tachan, Sven Rühle *, Arie Zaban

Institute of Nanotechnology & Advanced Materials, Department of Chemistry, Bar Ilan University, Ramat Gan 52900, Israel

ARTICLE INFO

Article history:
Received 13 May 2009
Received in revised form
5 October 2009
Accepted 5 October 2009
Available online 1 November 2009

Keywords:
Dye-sensitized solar cells
Dye-sensitized solar tubes
FTO synthesis
Spray pyrolysis
Current collector
Sealing

ABSTRACT

A dye-sensitized solar cell (DSSC) fabricated inside a glass tube to form a dye-sensitized solar tube (DSST) is presented. We developed the synthesis of Fluorine-doped Tin oxide (FTO) with a high optical transmittance and low sheet resistance, which was deposited inside a glass tube by spray pyrolysis. The FTO was covered with a mesoporous TiO_2 film using electrophoretic deposition (EPD). Subsequently the tube was sintered, sensitized with a Ru-dye (N3) and immersed into redox electrolyte while a Pt-coated rod closed the electrical circuit. Sealing of DSSCs is still a major problem. The new design reduces significantly the area that requires sealing compared to conventional flat cells, moreover sealing of a tube is significantly simpler than two flat plates. A huge advantage of the tube design is the possibility to incorporate a current collector without blocking direct sunlight from entering the cell. Panels consisting of DSSTs allow air flow in between the tubes, thus decreasing the wind resistivity while the cylindrical shape of the DSST can be used to collect diffuse light more effectively. Initial results on a prototype show a light to electric power conversion efficiency of 2.8%, demonstrating the feasibility of the new tube concept.

1. Introduction

Dye-sensitized solar cells (DSSC) based on nanocrystalline mesoporous TiO_2 films have attracted much attention as a potential low-cost alternative for single- or polycrystalline p–n junction silicon solar cells. DSSCs can reach solar to electrical energy conversion efficiencies above 10% [1]. Upon illumination photons are absorbed by dye molecules, which inject electrons from their excited states into the conduction band of the TiO_2 nano-particles. Oxidized dye molecules are recharged by a redox electrolyte, which transports the positive charges by diffusion to a Pt counter electrode, while electrons diffuse through the TiO_2 network to a transparent conducting front electrode. The low-absorption coefficient of a dye monolayer is compensated by the mesoporous structure of the TiO_2 film, which leads to a strong increase in the number of TiO_2/dye/electrolyte interfaces through which photons pass, thus increasing the absorption probability. Best performance is usually achieved with the I^-/I_3^- redox couple dissolved in organic solvent while Fluorine-doped SnO_2 (FTO) is a widely used transparent conducting front electrode material with exceptional chemical stability.

Even though DSSCs are on the edge of commercialization a major challenge remains the sealing of the photo-electrochemical cell [2]. The high vapor pressure of the solvent and its capability to dissolve/destroy most sealing materials over time scales relevant for solar panels is a main obstacle for large-scale production. This problem has triggered the search for solid state or quasi solid state hole conductors, which can replace the liquid electrolyte without loss in performance. A number of materials such as inorganic wide bandgap hole conductors [3–6], hole conducting molecular solids [7], polymers [8], as well as ionic liquids [9–11] and gel-based electrolytes [12,13] have been investigated. However up to now it has not been possible to develop solid-state DSSCs with conversion efficiencies compatible with liquid electrolyte-based cells. Sealing remains a major challenge, especially in solar panels where individual cells are connected in series, which all have to be sealed separately.

A further disadvantage of the flat solar cell design is a reduced conversion efficiency due to the presence of a non-transparent conducting grid on the electrode facing the incident light, which is required for photocurrent collection. Alternative cell geometries have been proposed [14–17], however most of them involve a more complex cell design, which complicates cell fabrication.

Here we present a new and simple DSSC design based on tubes. Glass tubes were coated from the inner side with a conducting transparent FTO layer onto which the mesoporous TiO_2 film was deposited. A cross-section of these DSSTs is schematically shown in Fig. 1a. As counter electrodes we used FTO-coated glass rods, onto which a Pt layer was sputtered. The round shape of the DSSTs opened a way to transfer the opaque current collector to the backside of the cell, thus avoiding the losses associated with shading from collector lines (Fig. 1b). DSSTs drastically reduce the

* Corresponding author.
E-mail address: ruhles@mail.biu.ac.il (S. Rühle).

0927-0248/$ - see front matter © 2009 Elsevier B.V. All rights reserved.
doi:10.1016/j.solmat.2009.10.006

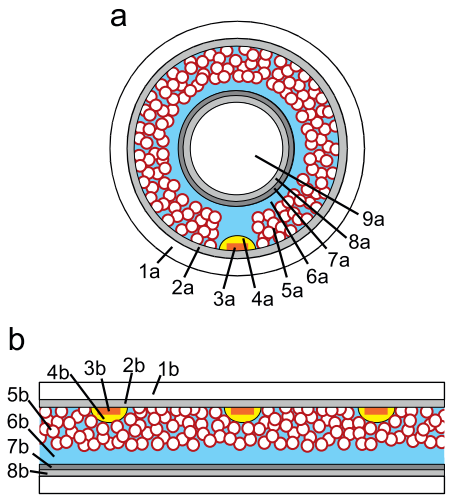

Fig. 1. (a) Schematic cross-section of a dye-sensitized solar tube (DSST) showing the glass tube (1a), the FTO layer deposited by spray pyrolysis (2a), a highly conducting current collector attached to the FTO on the bottom side inside the DSST (3a) and a polymer layer, which is protecting the current collector (4a). The mesoporous dye-sensitized TiO_2 film (5a) deposited onto the FTO is immersed into the redox electrolyte (6a). The circuit is closed by a counter electrode consisting of a sputtered Pt layer (7a) on top of a sprayed FTO film (8a), deposited onto a quartz rod (9a). (b) Schematic drawing of a conventional dye-sensitized solar cell (DSSC) consisting of a flat glass substrate (1b), covered with commercial FTO (2b). The opaque current collector (3b) with a protective coating (4b) is partially blocking the incident light. The dye-sensitized TiO_2 film (5b) is immersed into electrolyte (6b) which is in contact with Pt (7b) deposited on flat FTO glass (8b).

area for sealing and can be used as building blocks for dye-sensitized solar panels in which individual cells (tubes) are easily mounted and replaced. We have produced a DSST and characterized a surface segment with an area of 0.7 cm^2 under direct illumination of simulated sunlight (AM1.5) to compare its performance to flat DSSCs.

2. Experimental

2.1. Materials

Tin (IV) chloride pentahydrate (98%), HF (40–45%), iodine (99.8%), *tert*-butylpyridine (99%), and potassium dichromate were purchased from Aldrich. Ethanol (absolute anhydrous) and sulfuric acid with a maximum water content of 0.1% were supplied by Gadot Lab Supplies Ltd. Acetone analytical was purchased from Frutarom Ltd., acetylacetone ($\geq$99.5%) and methoxypropionitrile were bought from Fluka, lithium iodide anhydrous and dimethylpropylimidazolium iodide came from Merck, and acetonitrile HPLC grade with a water content of 0.002% was purchased from J.T.Baker. TiO_2 nanopowder (P-25) was purchased from Degussa AG (Germany). The dye *cis*-dithiocyanato bis(4,4_-dicarboxylic acid-2,2_-bipyridine) ruthenium(II) commonly termed N3 was purchased from Dyesol (Australia). All chemicals were used as received without further purification.

2.2. FTO spray pyrolysis

For FTO spray pyrolysis 1 g of $SnCl_4 \cdot 5H_2O$ was dissolved in 20 ml ethanol and stirred vigorously for 3 h until the solution became transparent. Adding 0.14 ml of HF (40–45%) caused the solution to turn milky and continued stirring for 1 h was needed to get again a clear solution. In an alternative procedure all components were added together and treated in a sonication bath for 2 h until the solution appeared clear. In both cases the precursor solution was stirred further for 12–24 h before it was used for spray pyrolysis. This precursor was stable and could still be used weeks after preparation without any decrease in the conductivity of the resulting FTO films. Glass tubes with an inner diameter of 14 mm and a wall thickness of 0.8 mm were cut into 3 cm long pieces and cleaned with ethanol, mild soap and thoroughly rinsed with deionized water (18.2 MΩ), before they were inserted into dichromate acid solution, rinsed again with deionized water and dried in a filtered air stream. The glass tubes were inserted into a tube furnace using a homemade holder (see Fig. 2) and preheated to 550 °C. The precursor was atomized by a homemade glass nozzle using pulsed compressed air as a carrier gas (1 sec pulse duration and a 10 sec time interval in between pulses) to allow reheating of the substrate in between the pulses. Deposition was carried out from both sides of the tube to achieve a uniform deposition. FTO films were also deposited on flat glass substrates under identical deposition conditions to perform high-resolution scanning electron microscopy (HRSEM), atomic force microscopy (AFM) and optical transmission measurements without further complications due to the curved nature of the tube. Alternative preparation methods known from the literature were tested [18–20] but the described procedure produced films of highest quality.

2.3. Electrophoretic deposition (EPD)

EPD was used to produce micrometer thick mesoporous TiO_2 films [21,22] inside the FTO-coated glass tubes. TiO_2 nanoparticles (P-25) were mixed with 150 ml of ethanol and 0.4 ml of acetylacetone before the TiO_2 suspension was stirred with a magnetic stirrer for 15–72 h in a closed vessel. In a second beaker a solution of 35 mg iodine, 4 ml anhydrous acetone and 2 ml water were added to 100 ml of anhydrous ethanol and stirred with a magnetic stirrer. Just prior to EPD the TiO_2 suspension was added into the second beaker, followed by sonication for 10 min using an ultrasound processor (VCX-750 Sonics and Materials, Inc.) to homogenize the mixture while cooling the suspension in an ice bath. For the EPD the FTO-coated glass tube and a Pt wire, placed in the center of the tube, served as electrodes. The EPD was performed at constant current using a Keithley 2400 source meter. The current was applied for 20 sec before the film was dried at 130 °C for 10 min to avoid cracking and pinholes, which are

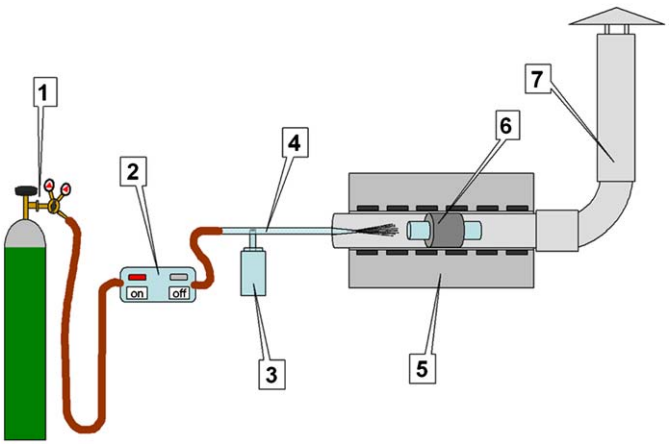

Fig. 2. Schematic drawing of the spray pyrolysis system, showing the gas cylinder with compressed air (1), an automatic shutter (2), the precursor solution (3), a spray nozzle (4), a tube furnace (5), the specially designed glass tube holder (6) and the exhaust (7).

caused by organic residues. After applying the deposition cycle six times a surface area of approximately 6 cm^2 was homogeneously covered with a mesoporous TiO_2 film. To characterize the solar cell performance of a tube segment the film area was reduced to approximately 1 cm^2 and the excessive TiO_2 film was mechanically scraped off. After sintering for 1 h at 550 °C the porous TiO_2 tube electrodes cooled down to 80 °C and were immersed overnight into a 0.5 mM solution of N3 dye in ethanol.

2.4. Characterization methods

The morphology of the FTO films was investigated using a HRSEM (JEOL, 7000F) and an AFM (Multi-Mode V, Vecco). X-ray diffraction was performed using a Bruker D8 X-ray diffractometer with Cu K_α radiation (λ=1.5406 Å). Transmittance measurements were carried out in a Cary 500 scan UV–vis–NIR spectrophotometer (Varian, USA). The mesoporous TiO_2 film thickness was measured with a profilometer (Surftest SV 500). For solar cell measurements the dye-covered electrodes were rinsed with ethanol and dried under a filtered air stream. Afterwards a 5-mm-thin stripe of copper foil was attached to the FTO film at the bottom inside the glass tube to serve as a current collector, which was covered with Surlyn (DuPont) to protect it from the corrosive redox electrolyte and to prevent direct contact with the counter electrode. A special designed cell holder with an aperture area of 0.7 cm^2 was used to measure the performance of the mesoporous dye-sensitized TiO_2 film inside the tube. As a counter electrode a quartz rod was used, coated with Pt on top of an FTO layer. The composition of the electrolyte was: 0.6 M dimethylpropylimidazolium iodide, 0.1 M LiI, 0.05 M I_2, 0.5 M *tert*-butylpyridine in 1:1 acetonitrile–methoxypropionitrile. *I–V* characteristics were recorded with a potentiostat (Eco-Chemie) while the solar tube was illuminated in a Newport solar simulator (class A).

3. Results and discussion

3.1. FTO characterization

A HRSEM image of a sprayed FTO film with a sheet resistance of 10 Ω/square is shown in Fig. 3a (deposited at 550 °C onto a flat glass substrate). From the cross-section image, shown in Fig. 3b, we determine a film thickness of around 500 nm. An AFM image of sprayed FTO, scanned over an area of 5 μm × 5 μm is shown in Fig. 4, from which a surface roughness (Ra) of 13.7 nm is determined. The peaks in the XRD spectrum presented in Fig. 5 are typical for the tetragonal structure of SnO_2 [23,24]. Moreover we observe a high intensity of the (2 0 0) reflection, indicating a preferential growth direction [25]. Optical transmission spectra of bare and FTO-covered glass substrates are shown in Fig. 6. In the wavelength range 400–800 nm the spray-deposited FTO shows a transmittance of around 80%. Local maxima at 385, 455, 580 and 770 nm are caused by multiple reflections at the FTO/glass and FTO/air interface [26].

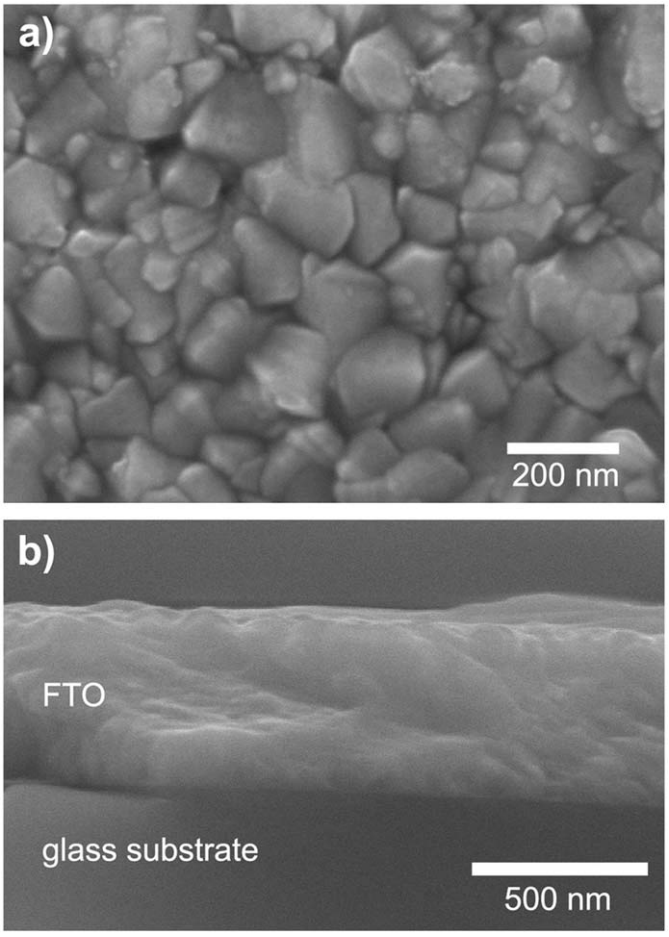

Fig. 3. (a) HRSEM image of an FTO film sprayed on a glass substrate at temperature of 550 °C. (b) Cross section HRSEM image showing an FTO film thickness of around 500 nm.

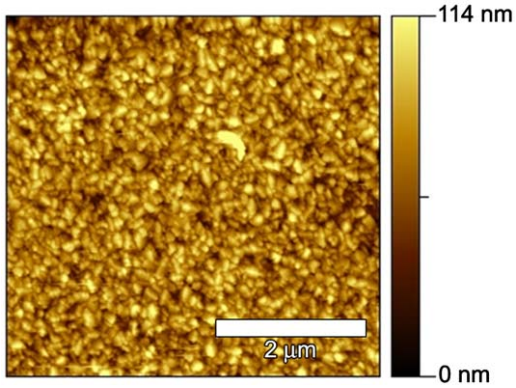

Fig. 4. AFM topography image of the spray pyrolysis deposited FTO film.

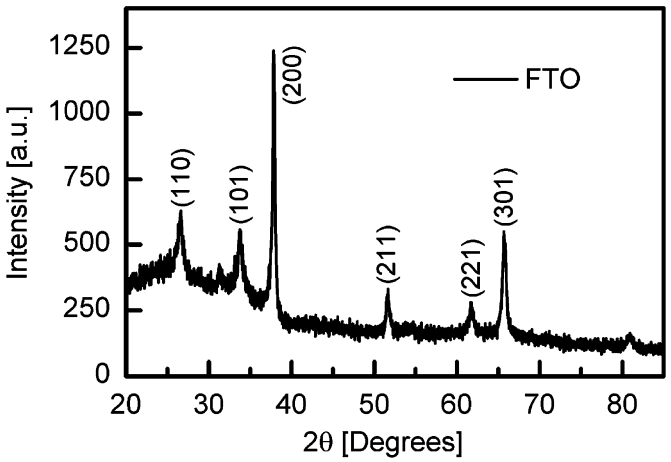

Fig. 5. XRD pattern of a spray pyrolysis-deposited FTO layer on glass.

Comparison with commercial FTO with a similar sheet resistance (TEC 8, with a sheet resistance of 8 Ω/square) reveals the excellent properties of the spray pyrolysis deposited films. The layer thickness of our spray pyrolysis deposited FTO films is significantly smaller than the thickness of TEC 8, which is typically 700 nm. The surface roughness of TEC 8 is with 36.4 nm much larger while its optical transmittance is lower compared to spray pyrolysis-deposited films, shown in Fig. 6. We note that spray pyrolysis of FTO is a process that provides films with very reproducible electrical and optical properties, excellent for DSSC application.

3.2. DSST assembly and characterization

Mesoporous TiO_2 films were deposited inside the FTO-coated tubes. To investigate the photovoltaic performance of the DSST, an area of 0.7 cm^2 was illuminated through a round aperture. A large fraction of the TiO_2 film was removed from the inside walls of the tubes to keep the solar cell area similar to the illuminated spot size. Fig. 7a shows a picture of the tube (1) with the dye-sensitized TiO_2 film (2) including the current collector made out of copper (3). The current collector was covered with a polymer foil (4) to prevent short circuiting with the counter electrode and to protect it against the I^-/I_3^- redox electrolyte. Fig. 7b shows the measurement system, consisting of the DSST (1–4), a quartz rod counter electrode, activated with a Pt layer on top of an FTO coating (5), the tube cell holder (6), the left and right flange with silicone O-rings to close and seal the cell (7) and the contact clamp to connect the counter electrode to the measurement system (8). A front view of a fully assembled DSST for *I–V* characterization is presented in Fig. 7c, showing the round illumination area. In the back view (Fig. 7d) one can see the copper tape, to which the measurement system was connected.

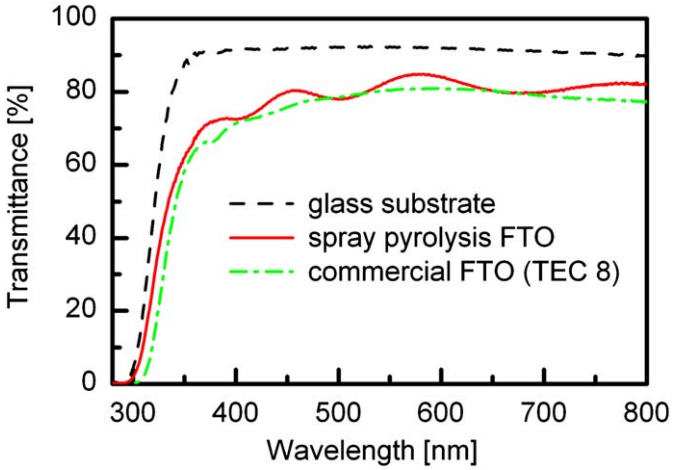

Fig. 6. Transmission measurements of a flat glass substrate (dashed) and an spray pyrolysis-deposited FTO film (solid). For comparison also the transmission of commercial FTO glass (TEC 8) is shown (dash-dotted).

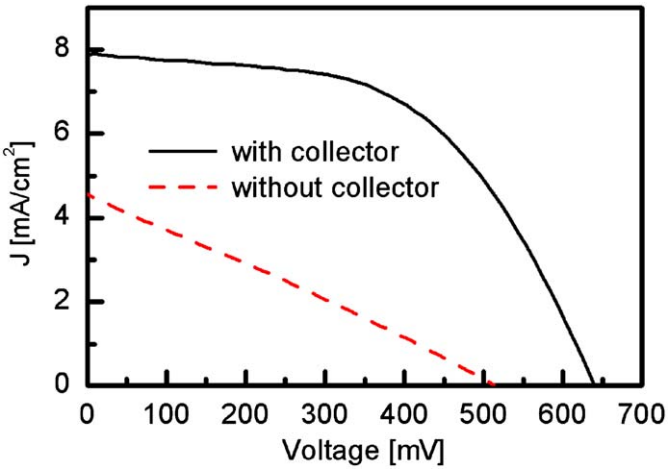

Fig. 8. Current–voltage characteristics of a DSST without current collector (dashed) and with a copper tape current collector, attached to the FTO substrate (solid). The solar cell parameters are summarized in Table 1.

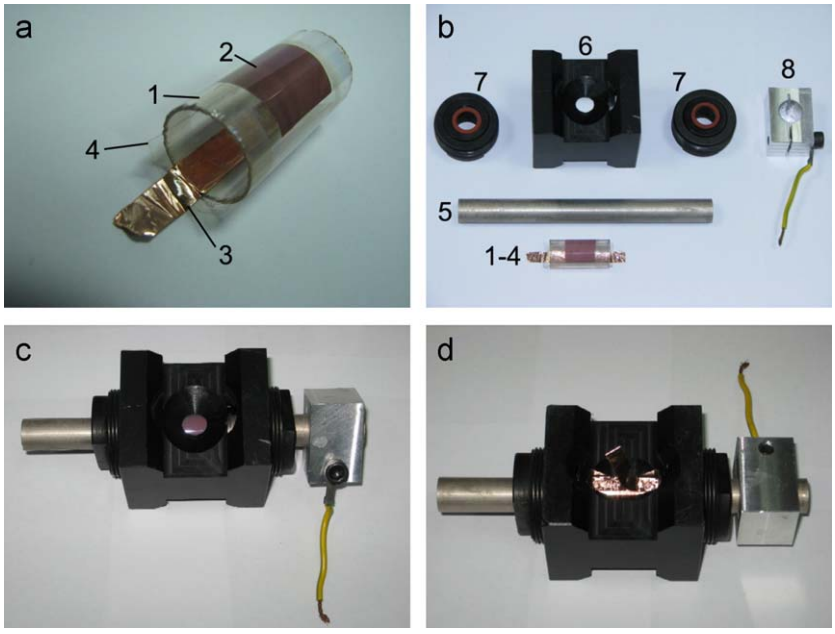

Fig. 7. (a) Photograph of a DSST, showing the glass tube (1), the dye-sensitized mesoporous TiO_2 film (2), the copper stripe current collector on the bottom side of the tube (3) and a transparent polymer film protecting the current collector (4). (b) Photograph of the DSST (1–4), the counter electrode rod (5), the tube holder (6), flanges including O-rings to close and seal the DSST (7) and an aluminum clamp to connect the counter electrode to the measurement system. (c) Front view of the assembled DSST. (d) Backside view of the DSST, showing the opening used to connect the current collector to the external circuit.

Table 1
Solar cell characteristics for a DSST with and without current collector.

	η [%]	V_{oc} [mV]	J_{sc} [mA/cm^2]	fill factor [%]
No current collector	0.7	514	4.6	28
Current collector	2.8	645	7.9	56

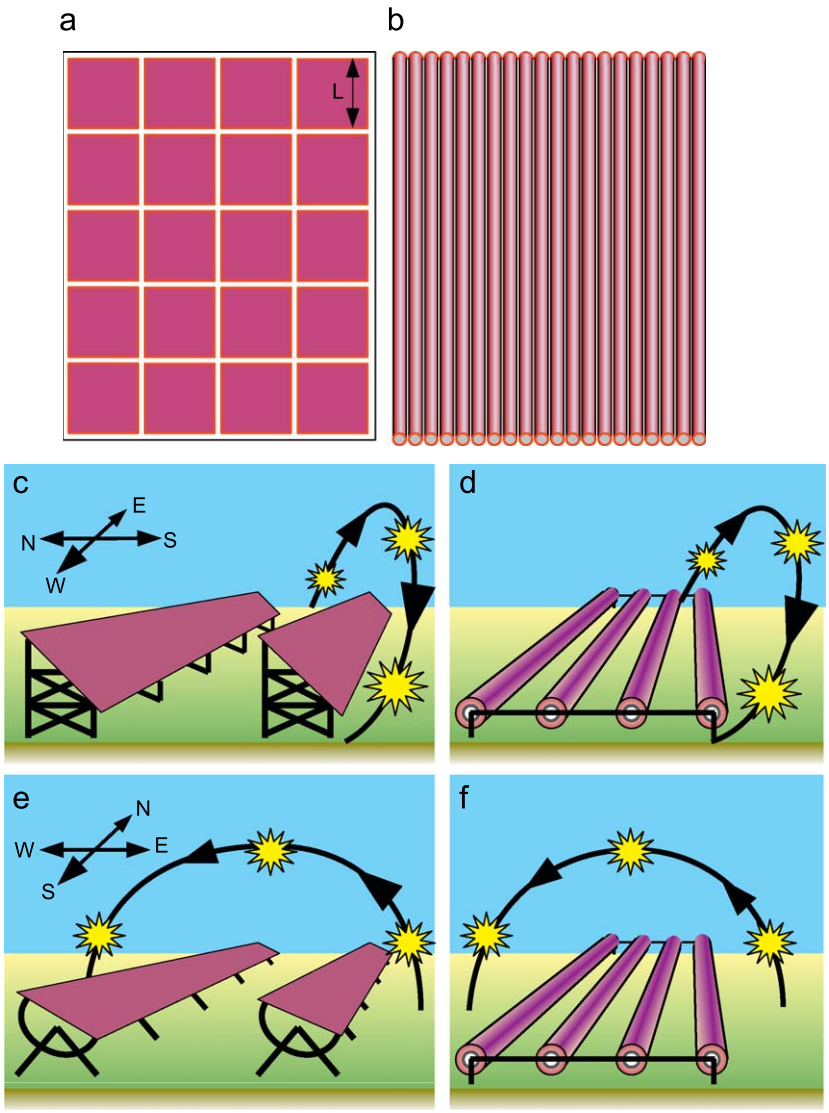

Fig. 9. (a) Solar panel consisting of 20 square DSSCs of side length *L*, which are individually sealed, shown by red lines. (b) Solar panel consisting of 20 DSSTs, showing the strongly reduced sealing area at the tube ends. (c) Required construction for solar panels on horizontal surfaces such as flat rooftops. (d) Simple construction of horizontally mounted DSSTs. (e) Sun-tracking of flat solar panels requires additional tracking hardware. (f) DSSTs do not require additional sun-tracking components due to the cylindrical geometry of the tubes.

I–V scans of a tube cell with and without current collector are shown in Fig. 8. For measurements without a current collector copper tape was connected to the FTO at the tube edges, but no copper tape was present inside throughout the DSST. Consequently the conversion efficiency was η=0.7% with a very low fill factor of 28%, which is characteristic for a large series resistance in the system, e.g. caused by the FTO sheet resistance in conjunction with large distances for current collection. With the current collector η increased to 2.8% and the fill factor improved to 56%, which demonstrates the impact of the sheet resistance and the importance of short paths to a highly conductive current collector. All DSST parameters for both systems, with and without current collector, are summarized in Table 1.

DSSTs have a number of intrinsic advantages over conventional flat DSSCs. A current collector can be mounted on the bottom side inside the tube, which is a significant advantage over flat system, where the current collector is mounted on the electrode facing the incident light. The latter reduces the conversion efficiency due to shading and limits the width and subsequently the length of the current collector grid lines. In DSSTs the collector line can be relatively thick/wide because it is located in a place where at best diffuse light is entering the cell, thus keeping light losses small.

The thick/wide collector lines can carry larger currents, which has the advantage that the cell can be scaled up by increasing its length while the area that requires sealing at both tube ends remains constant. Fig. 9a and b compares the sealing area of dye-sensitized solar panels based on flat DSSCs and tube cells. The example in Fig. 9a shows a solar panel consisting of 20 square DSSCs (with a side length L), which have to be sealed individually, leading to a total sealing length of 80 L. Fig. 9b shows a panel of same size consisting of 20 DSSTs with a sealing length of $8\pi L \approx 25$ L, which is less than a third. The sealing area ratio of tube cell-based panels to flat systems decreases further when the number of individual solar cells per panel is increased. Besides the smaller sealing area DSSTs have the inherent advantage that it is technologically much simpler to seal a tube than a flat system.

The tube panel design has the additional advantage that incident light approaching the surface under an angle can be efficiently collected with horizontally mounted tube arrays, e.g. on flat rooftops. Fig. 9c shows the required construction for flat solar panels to collect efficiently light under some incidence angle, while a horizontal module design based on DSSTs is shown in Fig. 9d. Shading of neighboring tubes is avoided keeping a distance in between them, providing a simple installation. Fig. 9e and f show that DSSTs have similar properties like flat panels in conjunction with a sun tracking mechanism when the tubes length axis is oriented in the north–south direction. The DSSTs convert the light effectively over a large range of incident angles. Furthermore DSSTs collect more diffuse light and an improved cell cooling is warranted by the surrounding air. The tube design allows a quick and easy replacement of individual tubes, thus keeping maintenance costs low. The presented conversion efficiency of 2.8% demonstrates the feasibility of the tube concept. Further development of the materials and fabrication processes should lead to higher efficiencies and has the potential of lower production costs compared to commercial DSSCs.

4. Conclusions

A dye-sensitized solar tube with a light-to-electric power conversion efficiency of 2.8% was produced. To achieve that goal, conducting FTO films were produced by spray pyrolysis inside glass tubes, with electrical and optical properties compatible with commercial FTO. The tube geometry has the huge advantage that the sealing area is significantly smaller compared to the conventional flat solar cell design. Furthermore the sealing of tubes can technologically be much simpler realized compared to the edges of flat glass sheets. This is of particular importance for dye-sensitized solar panels, in which individual cells are connected in series. Additionally the tube geometry allows the use of current collectors without loss of active solar cell area that is exposed to direct sunlight.

Acknowledgements

The authors acknowledge financial support from the Israeli Science Foundation (Bikura program). SR acknowledges financial support from the European Union within the FP7 framework (Marie Curie Intra-European Fellowship for Career Development). The authors are thankful for the technical support provided by Menahem Schneeberg.

Appendix A. Supplementary data

Supplementary data associated with this article can be found in the online version at doi: 10.1016/j.solmat.2009.10.006.

References

[1] M.A. Green, K. Emery, Y. Hishikawa, W. Warta, Solar cell efficiency tables (version 33), Prog. Photovoltaics 17 (2009) 85–94.
[2] A. Hinsch, S. Behrens, M. Berginc, H. Bönnemann, H. Brandt, A. Drewitz, F. Einsele, D. Fassler, D. Gerhard, H. Gores, R. Haag, T. Herzig, S. Himmler, G. Khelashvili, D. Koch, G. Nazmutdinova, U. Opara-Krasovec, P. Putyra, U. Rau, R. Sastrawan, T. Schauer, C. Schreiner, S. Sensfuss, C. Siegers, K. Skupien, P. Wachter, J. Walter, P. Wasserscheid, U. Würfel, M. Zistler, Material development for dye solar modules: results from an integrated approach, Prog. Photovoltaics 16 (2008) 489–501.
[3] B. O'Regan, D.T. Schwartz, Efficient dye-sensitized charge separation in a wide-band-gap p-n heterojunction, J. Appl. Phys. 80 (1996) 4749–4754.
[4] V.P.S. Perera, K. Tennakone, Recombination processes in dye-sensitized solid-state solar cells with CuI as the hole collector, Sol. Energy Mater. Sol. Cells 79 (2003) 249–255.
[5] K. Tennakone, G.K.R. Senadeera, D.B.R.A. De Silva, I.R.M. Kottegoda, Highly stable dye-sensitized solid-state solar cell with the semiconductor 4CuBr $3S(C_4H_9)_2$ as the hole collector, Appl. Phys. Lett. 77 (2000) 2367–2369.
[6] B. O'Regan, F. Lenzmann, R. Muis, J. Wienke, A solid-state dye-sensitized solar cell fabricated with pressure-treated P25-TiO_2 and CuSCN: Analysis of pore filling and IV characteristics, Chem. Mater. 14 (2002) 5023–5029.
[7] U. Bach, D. Lupo, P. Comte, J.E. Moser, F. Weissortel, J. Salbeck, H. Spreitzer, M. Grätzel, Solid-state dye-sensitized mesoporous TiO_2 solar cells with high photon-to-electron conversion efficiencies, Nature 395 (1998) 583–585.
[8] J. Xia, N. Masaki, M. Lira-Cantu, Y. Kim, K. Jiang, S. Yanagida, Effect of doping anions' structures on poly (3,4-ethylenedioxythiophene) as hole conductors in solid-state dye-sensitized solar cells, J. Phys. Chem. C 112 (2008) 11569–11574.
[9] R. Kawano, H. Matsui, C. Matsuyama, A. Sato, M.A.B.H. Susan, N. Tanabe, M. Watanabe, High performance dye-sensitized solar cells using ionic liquids as their electrolytes, J. Photochem. Photobiol. A 164 (2004) 87–92.
[10] W. Kubo, T. Kitamura, K. Hanabusa, Y. Wada, S. Yanagida, Quasi-solid-state dye-sensitized solar cells using room temperature molten salts and a low molecular weight gelator, Chem. Commun. (2002) 374–375.
[11] E. Stathatos, P. Lianos, S.M. Zakeeruddin, P. Liska, M. Grätzel, A quasi-solid-state dye-sensitized solar cell based on a sol-gel nanocomposite electrolyte containing ionic liquid, Chem. Mater. 15 (2003) 1825–1829.
[12] P. Wang, S.M. Zakeeruddin, J.E. Moser, M.K. Nazeeruddin, T. Sekiguchi, M. Grätzel, A stable quasi-solid-state dye-sensitized solar cell with an amphiphilic ruthenium sensitizer and polymer gel electrolyte, Nat. Mater. 2 (2003) 402–407.
[13] J. Shi, S. Peng, J. Pei, Y. Liang, F. Cheng, J. Chen, Quasi-solid-state dye-sensitized solar cells with polymer gel electrolyte and triphenylamine-based organic dyes, A.C.S. Appl. Mater. Interfaces 1 (2009) 944–950.
[14] X. Fan, F. Wang, Z. Chu, L. Chen, C. Zhang, D. Zou, Conductive mesh based flexible dye-sensitized solar cells, Appl. Phys. Lett. 90 (2007) 073501-3.
[15] L. Yong, S. Hui, D. Youjun, A novel solar cell fabricated with spiral photo-electrode for capturing sunlight 3-dimensionally, Sci. China 49 (2006) 663–673.
[16] S. Rühle, S. Greenwald, E. Koren, A. Zaban, Optical waveguide enhanced photovoltaics, Opt. Express 16 (2008) 21801–21806.
[17] X. Fan, Z.Z. Chu, F.Z. Wang, C. Zhang, L. Chen, Y.W. Tang, D.C. Zou, Wire-shaped flexible dye-sensitized solar cells, Adv. Mater. 20 (2008) 592–595.
[18] X. Zhi, G. Zhao, T. Zhu, Y. Li, The morphological, optical and electrical properties of SnO_2:F thin films prepared by spray pyrolysis, Surf. Interface Anal. 40 (2008) 67–70.
[19] R. Riveros, E. Romero, G. Gordillo, Synthesis and characterization of highly transparent and conductive SnO_2:F and In_2O_3:Sn thin films deposited by spray pyrolysis, Braz. J. Phys. 36 (2006) 1042–1045.
[20] T. Kawashima, H. Matsui, N. Tanabe, New transparent conductive films: FTO coated ITO, Thin Solid Films 445 (2003) 241–244.
[21] S. Dor, S. Rühle, A. Ofir, M. Adler, L. Grinis, A. Zaban, The influence of suspension composition and deposition mode on the electrophoretic deposition of TiO_2 nanoparticle agglomerates, Colloids Surf. A 342 (2009) 70–75.
[22] L. Grinis, S. Dor, A. Ofir, A. Zaban, Electrophoretic deposition and compression of titania nanoparticle films for dye-sensitized solar cells, J. Photochem. Photobiol. A. 198 (2008) 52–59.
[23] E. Elangovan, M.P. Singh, K. Ramamarthi, Studies on structural and electrical properties of spray deposited SnO_2:F thin films as a function of film thickness, Mater. Sci. Eng. B 113 (2004) 143–148.
[24] B. Russo, G.Z. Cao, Fabrication and characterization of fluorine-doped thin oxide thin films and nanorod arrays via spray pyrolysis, Appl. Phys. A.: Mater. Sci. Process. 90 (2007) 311–315.
[25] A.V. Moholkar, S.M. Pawar, K.Y. Rajpure, S.N. Almari, P.S. Patil, C.H. Bhosale, Solvent-dependent growth of sprayed FTO thin films with mat-like morphology, Sol. Energy Mater. Sol. Cells 92 (2008) 1439–1444.
[26] R. Swanepoel, Determination of the thickness and optical constants of amorphous silicon, J. Phys. E.: Sci. Instrum. 16 (1983) 1214–1222.